Sakarya University Journal of Computer and Information Sciences
http://saucis.sakarya.edu.tr/

DOI: 10.35377/saucis...1233094 RESEARCH ARTICLE

Analysis of Urine Sediment Images for Detection and Classification of Cells

Hilal Atıcı[1], H. Erdinç Koçer[2], Abdullah Sivrikaya[3], Mehmet Dağlı[3]

[1]Department of Computer Engineering, Selcuk University, Konya / Türkiye
[2]Department of Electrical and Electronics Engineering, Selcuk University, Konya / Türkiye
[3]Department of Biochemistry, Selcuk University Faculty of Medicine, Konya / Türkiye

Corresponding author:
Hilal Atıcı, Department of Computer Engineering, Selcuk University
E-mail address: hilalatici@eskisehir.edu.tr

Received: 17 January 2023
Revised: 02 March 2023
Accepted: 17 March 2023
Published Online: 30 April 2023

Citation: Atıcı H. et al. (2023). Analysis of Urine Sediment Images for Detection and Classification of Cells. *Sakarya University Journal of Computer and Information Sciences*.6 (1) https://doi.org/10.35377/saucis...1233094

ABSTRACT

Urine sediment tests are important in diagnosing abnormal diseases related to the urinary tract. The formation of cells such as red blood cells and white blood cells in the urine of patients is important for diagnosing the disease. Therefore, cells need to be fully identified in clinical urinalysis. Urinalysis with human eyes; since it is subjective, time consuming and causing errors, methods have been developed to automate microscopic analysis with the help of image processing. In this study, a deep learning algorithm (Yolov7), which gives successful results in image processing technology, was used as a method. The dataset used in the study was created by using microscopic images of urine sediment taken from the Biochemistry Laboratory of the Faculty of Medicine, Selcuk University. Seven different cell segmentation and classification studies have been carried out, including WBC, RBC, WBCC, Epithelial, Flat Epithelial, Mucs and Bubbles, which have clinical value for diagnosing the disease. Experimental studies were carried out with the Yolov7 algorithm, and the results were presented. As a result of the experiment, the urine cell images were segmented into cells using the deep learning method. The segmentation performance metrics, precision, recall, mAP(0.5) and F1-Score(%) were calculated as 0.384, 0.759, 0.432 and 0.510, respectively. The segmented cells were classified as WBC, RBC, WBCC, Epithelial, Flat Epithelial, Mucs and Bubbles and the classification accuracies were obtained as 0.78, 0.94, 0.90, 0.57, 0.92, 0.68 and 0.97, respectively. A mean classification success of 0.822 was achieved for all classes. Thus, it has been seen that the Yolov7 model can be used by experts as a tool for recognizing cells in the urine sediment. Consequently, it has been shown that suitable deep-learning models can be used to recognize the biometric properties of urinary sediment cells. With the model created using deep learning libraries, urine sediment cells can be easily classified, and it is possible to define many different cells if there is a dataset with a sufficient number of images.

Keywords: Deep learning, urine sediment, classification, segmentation

1. Introduction

Today, the microscope is used by technicians in many laboratories to detect cells or parasites. Urine sediment tests are important in diagnosing abnormal diseases related to the urinary tract. The formation of red blood cells, white blood cells, crystals, bacteria, and other microorganisms in the urine sediments of patients is of great importance for diagnosis.

In 2010, the development of an automatic recognition and counting system for visual components of urine sediment was worked on. With the help of image processing technology, image segmentation, representation and definition, geometric properties and texture properties were obtained. The findings of the experiments showed that the ability to learn and classify the neural network could be effectively improved by combining genetic algorithms with appropriate feature selection [1].

In 2013, a study was conducted on the detection and segmentation of red blood cells and white blood cells in urine sediment images. The algorithm process consists of three main parts. The first step is the segmentation of the urine sediment analysis using a Neural Network applied to the HSV color model image. The next step is to remove the noise with morphology operations. The final step is to detect RBCs and WBCs using the Circle Hough Transform. Experimental results showed the mean error percentage of RBC and WBC detection as 5.28 and 8.35, respectively [2].

In a study conducted in 2014; A comprehensive approach was introduced for detecting microscopic urine particles. Microscopic images include RBC, WBC, Calcium oxalate, Triple phosphate and other cells. 16 shape descriptors and 38 textural features were extracted. When K-NN, Neural Network, Naive Bayes, Decision Tree, and Rule Induction classifiers were tested with 10-fold cross-validation, the evaluation resulted in 96.41% accuracy performance with a minimum f measurement of 93.83% using the Neural Network [3].

A 2017 study focused on automatically identifying malaria-infected cells using deep learning methods. Thin blood images were used to compile a dataset of malaria-infected red blood cells and uninfected cells, labeled by a group of four pathologists. Three types of well-known neural networks were evaluated, namely LeNet, AlexNet, and GoogLeNet. The simulation results showed that all these deep convolutional neural networks achieve classification accuracies of over 95%, higher than the approximately 92% accuracy obtained using the support vector machine method. Moreover, deep learning methods have the advantage of being able to automatically learn features from input data, thus requiring minimal input from human experts for automated malaria diagnosis [4].

Urine sediment examination is an important topic in kidney disease analysis and is often a prerequisite for subsequent diagnostic procedures. In a study conducted in 2018, the DFPN (Feature Pyramid Network with DenseNet) method was proposed to overcome the problem of class confusion in urinary sediment examination images. The urine sediment examination dataset contains 42759 labeled samples in a total of 5377 images and includes 7 cell categories: cast, crystals, epithelium, epithelial nucleus, erythrocyte, leukocytes, and mycete. The importance of two parts of the basic model for urinary sediment examination cell detection was investigated. First, adding the attention module at the beginning of the network and the class-specific attention module increased the mAP by 0.7 points with the pre-trained ImageNet model and 1.4 points with the pre-trained COCO model. Next, DenseNet was introduced to the base model (DFPN) for cell detection in urine sediment examination. The DFPN achieved the best result with a mAP of 86.9% on the urine sediment examination test set after balancing between loss of classification and loss of bounding box regression [5].

Urine cast cells are a particularly important examination material in clinical urinalysis for disease diagnosis. Therefore, the exact identification of cells in clinical urinalysis is of great importance. A 2019 study proposes an effective approach for cast cell detection and recognition in urine sediment images. Urine cast cells were used as detection targets in urine microscopy, and then the ResNet50 network was used. Finally, the target area feature maps for classification and localization were entered into the classification subnet and the regression subnet separately, and the detection results were obtained. The data took only 0.2s per image on the NVIDIA Titan X GPU, with the average precision of the recognition result being %89.4 [6].

In 2019, a study was conducted on image classification using microscopic images of urine sediment. A total of 1670 datasets are used for training and testing different convolutional network models in deep learning. These models are VGG 16, VGG 19, Resnet 50, InceptionV3, Xception, Inception-ResnetV2 and MobileNet. Classification of urine sediment has been successfully applied. In the study, the following were evaluated for these models: confusion matrix, loading, feature extraction and average feature extraction times, accuracy, precision, recall and f-scoring. The models that give the best results through these evaluations are Inception V3 and Inception-Resnet V2. The highest accuracy (99.4%) was also obtained with these models. However, MobileNet achieved remarkable results with 98% accuracy, considering its very light size of 16.82 MB compared to Inception-Resnet V2 of 219.93 MB [7].

2. Material and Method

In this study, the Yolov7 model, which is a machine learning-based algorithm that was previously trained with the COCO dataset, was used. To implement the software, Google Colaboratory Pro [8], Tesla T4 graphics card and Pytorch library were used.

2.1 Yolov7 (You Only Look Once) deep learning model

By looking at the images, people can instantly understand which objects are in the images, their positions, and their interactions with each other. The human visual system works very quickly and accurately. Fast and highly accurate algorithms in object detection have allowed computers to drive without special sensors, and assistive devices to transmit real-time scene information to users [9].

Unlike traditional object detection methods, YOLO has taken the finding of bounding boxes, calculation of class probabilities and all other operations as a single regression problem and brought a new view to the field of object detection. With YOLO, it is sufficient to look at the image only once to determine which objects are where on the image. Multiple bounding boxes are estimated simultaneously with a single convolutional network and class probabilities are estimated for each class. This combined model has several benefits over traditional object detection methods.

The YOLO detection model divides each image in training set into SxS(S=7) square cells (grid). If the center position of any objects to be detected is within any of the dividing cells, the cell where the center is located is responsible for detecting that object. Each cell generates the B bounding boxes and estimates the confidence score for these bounding boxes. The

confidence score reflects how confident the model is that the bounding box it produces contains an object and how accurate the probability that the produced bounding box is produced.

$$Confidence\ Score = P_r(Object) * IoU_{pred}^{truth} \quad (1)$$

It is calculated as Pr(Object)∈ (0,1). If there is no object in the dividing cells, the confidence score of those cells is 0, if there is, it is 1. Each cell also estimates the C conditional class probabilities Pr($Class$i $|Object$), as seen in equation 2. These possibilities are linked to cells containing objects. Regardless of the number of bounding boxes produced B, only one of the class probabilities per cell is estimated. Confidence scores are calculated on a class basis for each box by multiplying the conditional class probabilities and individual confidence score estimates during the test [10].

$$P_r(Class_i \mid Object) * P_r(Object) * IoU_{pred}^{truth} = P_r(Class_i) * IoU_{pred}^{truth} \quad (2)$$

Model	Test Size	AP^{test}	$AP_{50}{}^{test}$	$AP_{75}{}^{test}$	batch 1 fps	batch 32 average time
YOLOv7	640	51.4%	69.7%	55.9%	161 *fps*	2.8 *ms*
YOLOv7-X	640	53.1%	71.2%	57.8%	114 *fps*	4.3 *ms*
YOLOv7-W6	1280	54.9%	72.6%	60.1%	84 *fps*	7.6 *ms*
YOLOv7-E6	1280	56.0%	73.5%	61.2%	56 *fps*	12.3 *ms*
YOLOv7-D6	1280	56.6%	74.0%	61.8%	44 *fps*	15.0 *ms*
YOLOv7-E6E	1280	56.8%	74.4%	62.1%	36 *fps*	18.7 *ms*

Figure 1 YOLO Models [11]

Yolo v7 is the latest version of YOLO. Yolo v7 was released on July 7, 2022, by Wong Kin Yiu. This new version is Yolo's most accurate and fast real-time object detection version available. The Yolo frame has three parts, the Spine, the head and the neck. The spine detects important information in the image and sends this information from the neck to the head. The neck compiles information from the spine and creates feature pyramids. The head consists of the output layers and forms the last part of the structure. Yolov7 is not limited to one head. The auxiliary head assists the training in the middle tiers, while the auxiliary head is responsible for the final output. Additionally, to improve deep network training, a tag assignment mechanism was introduced that takes into account precision and network prediction results and then assigns tags. Among all real-time object detectors with 30 Fps or more, Yolov7 achieved the highest accuracy (56.8% AP). YOLOv7 was trained completely from scratch using the MS COCO [13] dataset without using any pre-trained weights [12].

2.2 Urine Sediment Dataset

This study was approved by the ethics committee of Selcuk University. (Number:2022/192, Date:12.04.2022). In this study, a dataset consisting of a total of 9,004 microscopic images of urine sediment obtained by using the DIRUI FUS-2000 device in the Biochemistry Laboratory of Selcuk University Medical Faculty Hospital was used. Segmentation and classification of cells found in microscopic urine sediment images in the dataset were emphasized. For this reason, each cell in the microscopic images in the dataset was labeled with the help of experts working in the Biochemistry Laboratory of Selcuk University Faculty of Medicine.

The dataset consists of seven classes: White Blood Cell (WBC), White Blood Cell Cluster (WBCC), Red Blood Cell (RBC), Epithelial, Flat Epithelial, Mucs and Bubbles. The images are 800 x 600 pixels in size in bmp format and have been labeled with the help of an expert. The images were obtained from the urine samples of the patients who came to the biochemistry laboratory. The obtained high-quality labeled dataset can be applied to machine learning and deep learning models to recognize different urine cell types, and the models can be trained and tested.

In order to apply the dataset to the Yolo algorithm, firstly, the labeling process was performed. The data labeling process was done with the MakeSense tool [14], which can be labeled online. The labeling process is important in terms of giving deep learning algorithms to the training set, where it can distinguish the desired objects and train itself.

The images in the Data Set were uploaded separately and the necessary labels were made. Seven classes in the dataset were added as labels. The cells in each image are marked with a rectangle and the class label to which they belong is selected. An image can also contain more than one cell. After all the labeling is done, the labeling file is exported. Since the dataset tag information uses tagging in Yolo format, it is exported in VOC XML format.

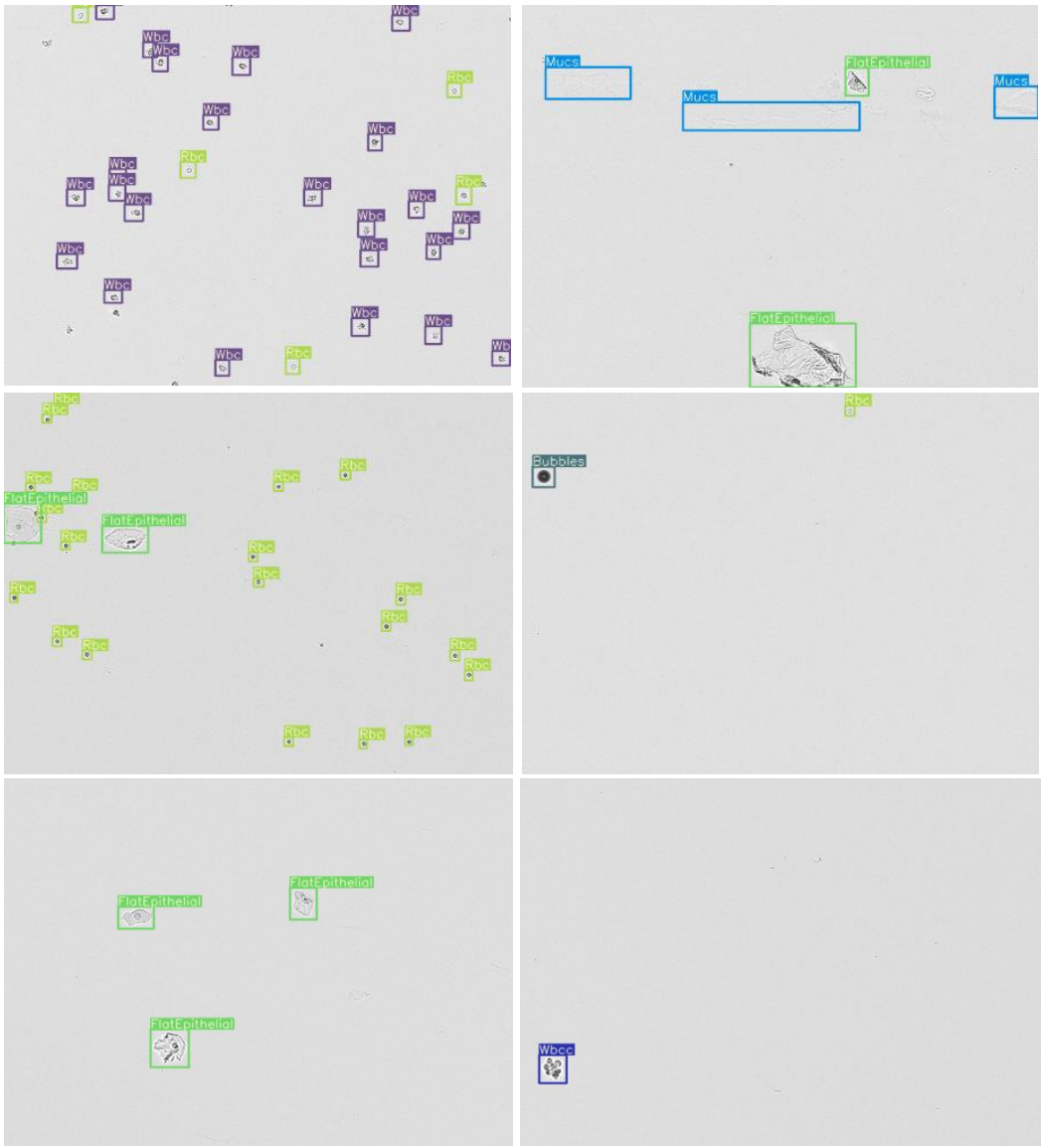

Figure 2 Labeled image examples.

2.2.1 Types of cells found in the data set

The dataset consists of seven classes: White Blood Cell (WBC), White Blood Cell Cluster (WBCC), Red Blood Cell (RBC), Epithelial, Flat Epithelial, Mucs and Bubbles.

Tablo 1 Cell Numbers and Types in each group

Cell Type	**Number of Cells**	**%**
RBC	16124	59,64
WBC	5980	22,12
Flat Epithelial	3574	13,22
Mucs	468	1,73
Epithelial	366	1,35
WBCC	309	1,14
Bubbles	212	0,78
Total	27,033	100

Leukocytes (White Blood Cells – WBC)

Leukocytes, known as white blood cells, play an active role in the body's fight against foreign substances, microbes and infectious diseases. A high incidence of these cells may indicate the presence of an infection or other underlying inflammatory medical problems associated with it.

Pathologically in the urine; more than normal leukocytes are seen in cases of urinary tract infection, kidney stone, kidney infection, urinary tract obstruction, blood diseases such as sickle cell anemia, pregnancy, some cancers such as bladder, kidney or prostate cancer, and consumption of some painkillers [15].

Red Blood Cells (RBC)

The presence of RBCs in the urine means that there is blood in the urine. Blood in the urine is medically referred to as hematuria. Although the sight of erythrocytes in the urine may sound scary, it is usually not life-threatening and can rarely be diagnosed due to serious illness. The presence of blood in the urine may be so small that it can only be diagnosed by looking under a microscope. But when it occurs, it is important to investigate the cause, because sometimes it can occur from several serious conditions [16]. Color change may occur in the urine due to some vitamin drugs or the consumption of carrots or citrus fruits. However, if there is visible bleeding in the urine, a physician should be consulted without delay and the treatment plan should be formed after the effect causing bleeding is found. It is quite normal for a normal person to have 0-3 erythrocytes in their urine. But if it is seen on it, it is useful to investigate the cause.

Among the causes of erythrocytes in the urine; having had a urinary tract infection, infection in the urinary bladder or kidneys, stones in the kidneys, bladder cancer, kidney cancer, glomerulonephritis, damage to the kidney, enlarged prostate, prostate cancer, tumor in the urinary tract, some painkillers, cancer drugs, kidney diseases that develop due to a genetic disease such as sickle cell anemia, inflammations caused by viruses, excessive exercise, blood clots can be counted [16].

Epithelial

Epithelial cells; are cells on the surface of various tissues of the body, especially blood vessels, organs, skin and urinary tract. Epithelial cells act as a barrier between the inside and outside of the body and protect the body against pathogens from outside. The surface of the urinary tract is also covered with epithelial cells. For this reason, it is considered normal to encounter a small number of epithelial cells in urinalysis. If the number of epithelial cells is less than 15-20 in the urine test, the epithelial cell test is considered normal in this urine test [17]. These parameters alone do not make sense. For this reason, a meaningful result can be obtained by looking at other parameters such as erythrocytes, leukocytes, parasites, and crystals in the blood.

Squamous Epithelium: It is the most common epithelial cell found in the urine. They are very large (largest cell seen in urine microscopy), small (very small compared to the cell) and mononuclear, with coarse cytoplasm, and flat, irregular borders. In some, double nuclei can be seen [18].

Renal Tubuler Epithelium: It is more common in urine with high protein content and casts. It is small, round, and polygonal. It is slightly larger than leukocytes and has a larger nucleus than granular and squamous epithelial cells. It is very similar to leukocytes in low-density urine [18].

Pathologically in the urine; In cases such as urinary tract infection, kidney stones, kidney infection, fungal infections, and bladder cancer, more epithelial cells are seen than normal [17].

Mucs

Mucus is a protective substance that covers and moistens the surfaces of structures such as the nose, trachea, urinary tract and stomach. It is normal to have a small number of mucus cells in the urine, while too many may indicate a urinary tract infection or other medical condition. The amount of mucus in the urine is determined by the urine test taken from the patient [19].

In the case of a normal discharge, little or moderate mucus cells are found in the urinalysis. A large number of mucus cells found in the urine may indicate medical conditions such as urinary tract infection, irritable bowel syndrome, kidney stones, and bladder cancer [19].

WBCC

It is formed by the coexistence of leukocytes, known as white blood cells. It is defined as leukocyte aggregation. Clusters of leukocytes are often seen in the urine of patients with urinary tract infections.

Bubbles

These cells are peculiar large cells with mononuclear cells that appear to contain one or more fluid-filled blebs. Air bubbles are very common due to air being trapped between the slide and the coverslip [20].

2.3 Performance measurements

There are many measurement criteria used to evaluate the performance of an object detection model. IoU (Intersection over Union), Precision, Recall, Average Precision (AP) and mean Average Precision (mAP) can be given as examples of the most used criteria.

IoU: IoU is an evaluation metric measuring the similarity between Ground Truth and model prediction. The metric is calculated as given in equation (3).

$$IoU = \frac{Area\ of\ Union}{\text{Area of intersection}} \tag{3}$$

Precision: Precision is calculated by dividing the correctly predicted positive samples against all predicted positive samples. The metric is calculated as given in equation (4).

$$Precision = \frac{TP}{(TP+FP)} \tag{4}$$

Recall: Recall is obtained by dividing the correctly predicted positive samples by all samples in the real class. The metric is calculated as given in equation (5).

$$Recall = \frac{TP}{(TP+FN)} \tag{5}$$

Average Precision (AP): AP is measurement metric that includes precision and recall metrics used to evaluate object detection performance. It is a number metric that summarizes the Precision-Recall curve by averaging the recall values from 0 to 1. The metric is calculated as given in equation (6).

$$AP = \frac{1}{11}\sum_{r\in(0,0.1,0.2,\ldots,1)} P_{interp(r)} \tag{6}$$

mAP: The mAP value is obtained by summing the APs of each class and dividing by the number of classes. The metric is calculated as given in equation (7).

$$mAP = \frac{1}{M}\sum_{j=1}^{M} AP_j \tag{7}$$

3. Experimental Results and Discussion

In this study, the machine learning-based deep learning-based YOLO algorithm, which was previously trained with the COCO dataset, was used. The YOLO algorithm is one of the one-step object detectors. There are six different models of Yolov7: Yolov7, Yolov7-X, Yolov7-W6, Yolov7-E6, Yolov7-D6 and Yolov7-E6E. In this study, the Yolov7 model was used. Because the Yolov7 model was trained with the COCO dataset and produced better results than other models. The Yolov7 model produced 161 fps (frame per second) and 2.8 ms results, surpassing other models. To implement the software, Google Colaboratory, Tesla T4 graphics card and Pytorch library, which provide access to powerful GPUs and do not require configuration, were used. In addition, to determine the error rates at the end of the training, the error rates were observed according to the iterations by using the Tensorboard graphical interface in the Tensorflow library. The training was completed after ***5 days 5 hours 29 minutes***.

Many experimental studies have been conducted to verify the performance of the YOLO-based model, and the results and findings have been analyzed. The training details used for the YOLOv7 model used in this study are presented in Table 2. These settings have been determined with the best results based on testing in the experimental studies conducted. In this study, various improvements have been made for test reviews and training by using the model developed on the open-source framework.

Table 2 Training Details of the Yolov7 Model

İnput Size	Model Parameters	Software Language	Environment	Library	Epoch	Batch Size	Optimizer	Activation Function
800x600	37228920	Python	Google Colaboratory	Torch	300	8	SGD	Leaky RELU & Sigmoid

In this study, the dataset used to train the network was created using microscopic images of urine sediment. To identify the cells in the training set of the network, the dataset was labeled by referring to the expert knowledge. The dataset is divided into three as training, validation and test set. The dataset consists of 9,004 images in total. These images contain a total of 27,033 cells.

The data set contains images of urine sediment and .xml files containing the location information of the cells in that image. However, to train the Yolov7 model, it is necessary to edit the dataset structure. Therefore, images (.jpg, .png etc.) and tags must be converted to .txt. In the format of Yolov7 tag (.txt) files, there is a line for each object, each line consists of class, x_center, y_center, width and height data. The box coordinates surrounding the object must be in the normalized x, y, w, h format (0–1). The classes in the dataset are zero-indexed. Therefore, the data has been converted to the Yolov7 tag file format.

Table 3 Comparison of performance metric results such as mAP, P and R obtained with the Yolov7 model for the validation set.

Class	Precision	Recall	mAP@.5
WBC	0.202	0.874	0.298
RBC	0.252	0.826	0.277
WBCC	0.296	0.583	0.264
Epithelial	0.395	0.507	0.419
FlatEpithelial	0.537	0.985	0.650
Mucs	0.264	0.594	0.270
Bubbles	0.744	0.946	0.848
All	0.384	0.759	0.432

Table 4 Comparison of performance metric results such as mAP, P and R obtained with the Yolov7 model for test set.

Class	Precision	Recall	mAP@.5
WBC	0.220	0.844	0.293
RBC	0.253	0.793	0.276
WBCC	0.303	0.483	0.265
Epithelial	0.438	0.479	0.420
FlatEpithelial	0.545	0.982	0.651
Mucs	0.299	0.479	0.257
Bubbles	0.760	0.865	0.840
All	0.403	0.704	0.429

P (Precision), R (Recall) and mAP (Average Precision) values give information about whether our model is performing well. The weight values obtained as a result of the training were recorded. These saved weights can be used later. For the experiment, the Yolo model was carried out for the segmentation of cells in the Urine Sediment image dataset. At the end of the experiment, Precision, Recall, mAP (0.5) and F1-Score(%)performance metrics were calculated as 0.384, 0.759, 0.432 and 0.510, respectively.

Table 5 Classification performance metric results with the Yolov7 model for test set

Class	WBC	RBC	WBCC	Epithelial	FlatEpithelial	Mucs	Bubbles	All
%Accuracy	%78	%94	%90	%57	%92	%68	%97	%82

In experimental studies carried out with the YOLO model; Classification accuracy for WBC, RBC, WBCC, Epithelial, FlatEpithelial, Mucs and Bubbles cells was calculated as %78, %94, %90, %57, %92, %68 and %97, respectively. A mean classification success of %82 was achieved for all classes. Obtained results are presented in Table 5.

Considering the results obtained, the detection accuracy of epithelial and mucus cells is lower than other cells. This is because; cell numbers are less, the colors of the cells are pale, and the edges are not clear and sharp. In particular, mucus cells are often confused with the background, as they have a flat and indistinct structure as seen in the pictures. The epithelial cell is

similar to Wbc cells, only larger in size, so it is mixed with Wbc cells. This problem can be solved by using more labeled mucus and epithelial cells.

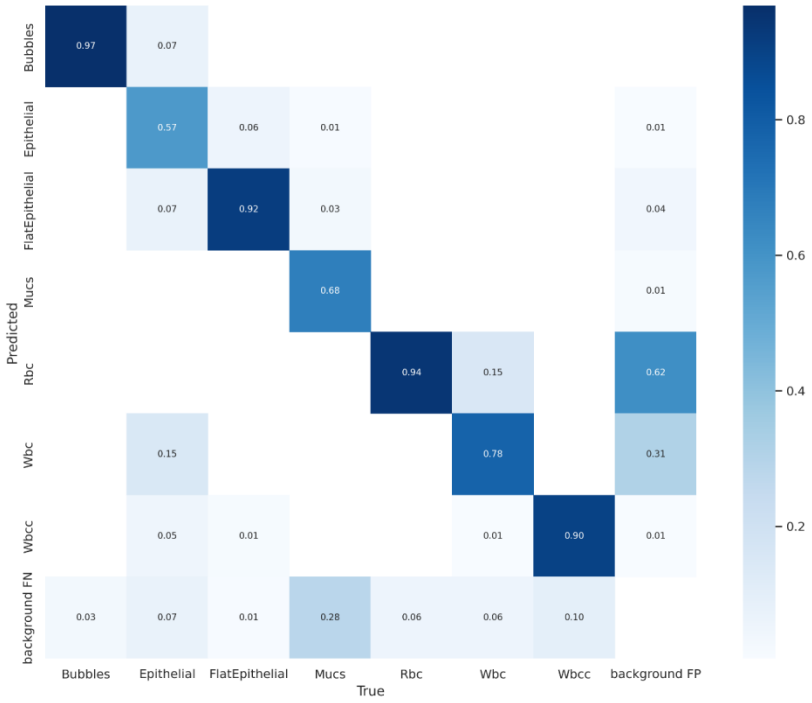

Figure 3 Confusion Matrix for Test Set

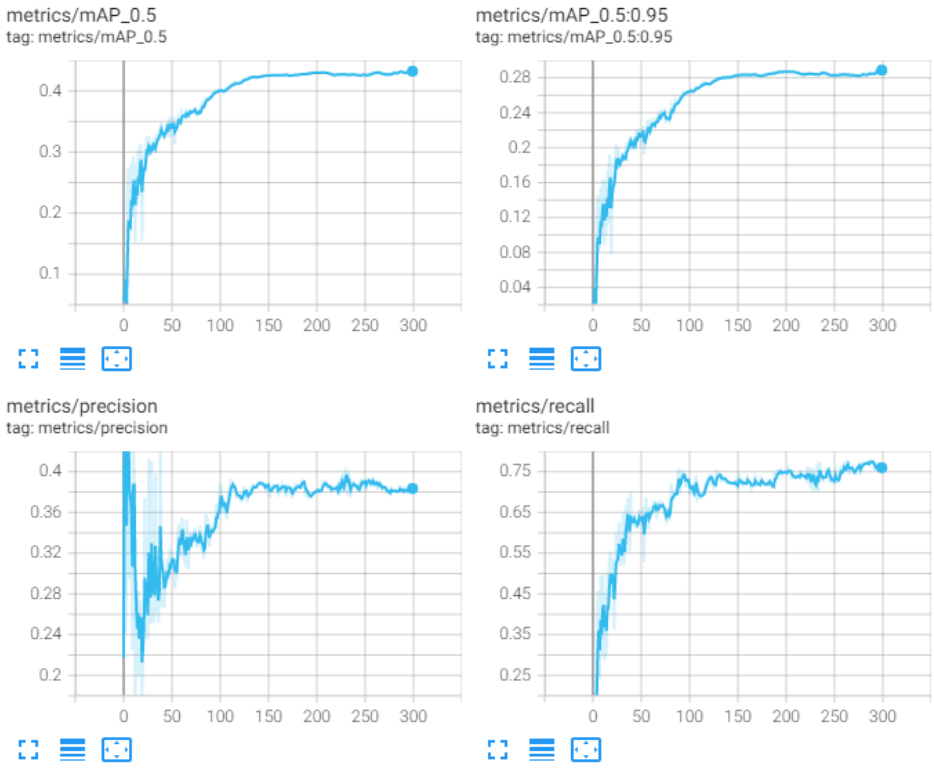

Figure 4 Plots of mAP_0.5, mAP_0.5:0.95, precision and recall values according to the epoch number during the training of the YOLOv7 network

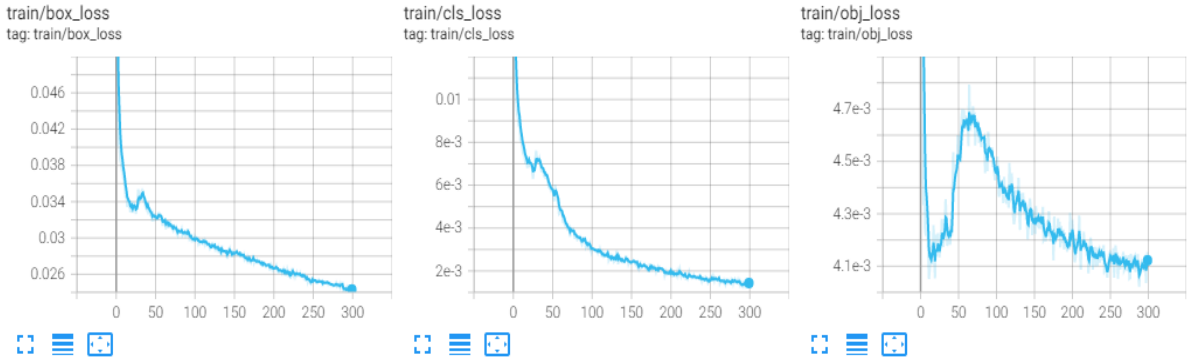

Figure 5 Plots of Box Loss, Class Loss and Object Loss values according to the epoch number during the validation of the YOLOv7 network

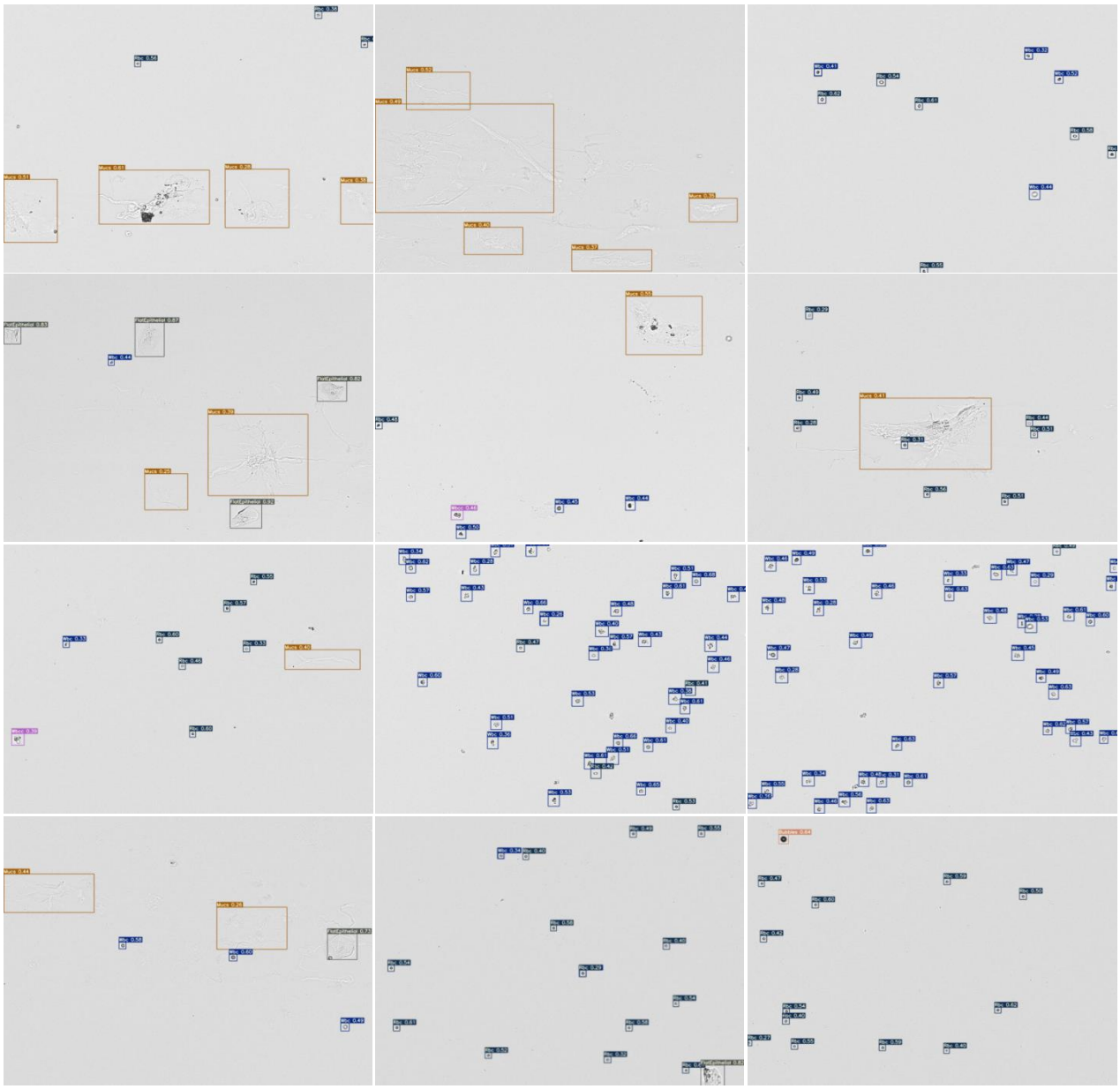

Figure 6 Test Image Samples

4. Conclusions

Analysis of microscopic images is used in many fields of medicine. Today, the microscope is used by technicians in many laboratories and anomalies (defects in the cell, parasites, low/excess cell count, etc.) are detected. Urine sediment tests are important in diagnosing abnormal diseases related to the urinary tract. The formation of red blood cells and white blood cells etc. in the urine sediments of patients is of great importance for diagnosing the disease. In patients' urine sediments, red blood cells, white blood cells, etc. the formation of cells is of great importance for diagnosing the disease. Therefore, cells need to be fully identified in clinical urinalysis. Urinalysis with human eyes; Since it is subjective, time consuming and causing errors, methods have been developed to automate microscopic analysis with the help of computer and software systems. In this study, the Yolov7 algorithm, which gives successful results in image processing technology, was used as a method and model. The dataset used in the study was obtained from the urine sediment microscopic images taken from the Biochemistry Laboratory of the Faculty of Medicine, Selcuk University. Studies have been conducted on seven different cell segmentation and classification, clinically valuable WBC, RBC, WBCC, Epithelial, Flat Epithelial, Mucs and Bubbles.

The contributions of this study can be summarized as follows. (1) It has been shown that urine sediment cells can be successfully classified with a deep-learning approach. (2) It has been observed that the Yolov7 model, which is frequently preferred in image processing applications, can be used as a means of recognizing cells in the urine sediment. (3) It has been seen that the labeling process is an important step in deep learning and recognition applications. (4) Since epithelial cells are similar to WBC cells, recognition success was low. Mucus cells, on the other hand, are perceived as background fluid due to their wide and diffuse appearance. Recognition percentage can be increased by increasing the number of sample images of cells with low classification success.

References

[1] X. Zhou, X. Xiao, and C. Ma. “A study of automatic recognition and counting system of urine-sediment visual components. ” *2010 3rd International Conference on Biomedical Engineering and Informatics*. Vol. 1. IEEE, 2010.

[2] W. Tangsuksant *et al.,* “Development algorithm to count blood cells in urine sediment using ANN and Hough Transform.” *The 6th 2013 Biomedical Engineering International Conference*. IEEE, 2013.

[3] M. D. Almadhoun and Alaa El-Halees. “Automated recognition of urinary microscopic solid particles.” *Journal of medical engineering & technology 38.2* (2014): 104-110.

[4] Y. Dong *et al.,* “Evaluations of Deep Convolutional Neural Networks for Automatic Identification of Malaria Infected Cells”, *2017 IEEE EMBS international conference on biomedical & health informatics (BHI).* IEEE, 2017.

[5] Y. Liang *et al.,* "Object detection based on deep learning for urine sediment examination.” *Biocybernetics and Biomedical Engineering 38.3* (2018): 661-670.

[6] Q. Li *et al.,* “A recognition method of urine cast based on deep learning.” 2019 International Conference on Systems, Signals and Image Processing (IWSSIP). IEEE, 2019.

[7] J.S. Velasco, M.K. Cabatuan, and E.P. Dadios, “Urine sediment classification using deep learning.” *Lecture Notes on Advanced Research in Electrical and Electronic Engineering Technology (2019)*: 180-185.

[8] Colab Pro, Available: https://colab.research.google.com/. [Accessed: 21.11.2022].

[9] J. Redmon *et al.,* “You only look once: Unified, real-time object detection.” *Proceedings of the IEEE conference on computer vision and pattern recognition*. 2016.

[10] P. F. Felzenszwalb *et al.,* “Object detection with discriminatively trained part-based models.” *IEEE transactions on pattern analysis and machine intelligence 32.9* (2009): 1627-1645.

[11] Chien-Yao Wang *et al.,* “YOLOv7: Trainable bag-of-freebies sets new state-of-the-art for real-time object detectors.” arXiv preprint arXiv:2207.02696 (2022).

[12] S. Ren *et al.,* “Faster r-cnn: Towards real-time object detection with region proposal networks.” *Advances in neural information processing systems 28* (2015).

[13] COCO Dataset. Available: https://cocodataset.org/#home, [Accessed: 20.05.2022].

[14] P. Skalski, “Make Sense,” 2019. Available: https://github.com/SkalskiP/make-sense/. [Accessed: 20.05.2022].

[15] Lökosit, Available: https://www.medicalpark.com.tr/lokosit/hg-2070. [Accessed: 21.11.2022].

[16] İdrarda RBC, Available: https://www.acibadem.com.tr/ilgi-alani/eritrosit-rbc/#genel-tanitim. [Accessed: 21.11.2022].

[17] İdrarda Epitel Nedir? Değeri Kaç Olmalı? Nedenleri ve Tedavisi, Available : https://saglik.li/idrarda-epitel-nedir/, [Accessed: 21.11.2022].

[18] Hücreler, Available: https://www.mustafaaltinisik.org.uk/idrar/turkce/hucre.htm, [Accessed: 21.11.2022].

[19] İdrarda Mukus Testi Nedir? Ne İşe Yarar?, Available: https://www.probiyotix.com/idrarda-mukus-testi-nedir-ne-ise-yarar/, [Accessed: 21.11.2022].

[20] S. E. Pambuccian, “Bedside Urinary Microscopy Giovanni Battista Fogazzi Lectures Series”, *Urinary Sediment: Part 6 and last: Contaminants and funny findings*, Milan, İtaly, March 8th, 2007.

Conflict of Interest Notice
The authors declare that there is no conflict of interest regarding the publication of this paper.

Ethical Approval and Informed Consent
It is declared that during the preparation process of this study, scientific and ethical principles were followed, and all the studies benefited from are stated in the bibliography.

Availability of data and material
Not applicable

Plagiarism Statement
This article has been scanned by iThenticate ™.